Use of Two-Dimensional Stress in the Modelling of Guided Wave Generation by Circular Piezoceramics

Nicolas Quaegebeur, Pierre Claude Ostiguy, Patrice Masson

7th European Workshop on Structural Health Monitoring
July 8-11, 2014. La Cité, Nantes, France

USE OF TWO-DIMENSIONAL STRESS IN THE MODELLING OF GUIDED WAVE GENERATION BY CIRCULAR PIEZOCERAMICS

Nicolas Quaegebeur, Pierre-Claude Ostiguy, Patrice Masson

GAUS, Dept of Mechanical Engineering, Université de Sherbrooke, Sherbrooke, QC, J1K 2R1, Canada

nicolas.quaegebeur@usherbrooke.ca

ABSTRACT

Traditional transducer design methods in Structural Health Monitoring based on Guided Wave propagation rely on the use of the pin-force model, assuming that a piezoelectric actuator can be modelled as a constant shear stress applied at its edge, whatsoever the frequency generated. However, the assumptions of this model are only validated for infinitely thin piezoelectric elements, weak coupling between the host structure and the transducer, and when the wavelength of the generated guided wave is above the size of the transducer. In this paper, a three-dimensional analysis of guided wave generation by a circular piezoceramic is proposed, taking into account the complex shear and normal interfacial stress profile between the transducer and the host structure. The complex stress profile is extracted from a Finite Element Model and then used as a parameter in the analytical propagation formulation. The influence of piezoceramic actuator dimension, thickness and host structure properties is then assessed numerically.

KEYWORDS : *guided waves, transducer, piezoceramics, propagation model, Finite Element Model (FEM)*

INTRODUCTION

Among the available technologies, Structural Health Monitoring (SHM) systems based on guided wave generated and sensed using an array of piezoceramic transducers offer a low footprint, cost-effective and reliable method for a quick and continuous monitoring of metallic, composite structures or assemblies [1]. Classical methods use sparse or compact transducers arrays mounted onto the structure and the inspection is performed using pitch-and-catch approach, electro-mechanical impedance changes or pulse-echo measurements. For pitch-and-catch or pulse-echo approaches, the propagation and interaction of guided waves with potential damage is exploited and measured echoes can be detected and analyzed using signal processing or imaging algorithms [2]. In this case, the optimal transducers configuration in terms of size, material, thickness and location relies on the precise modelling of guided wave generation by a piezoceramic transducer of finite dimension for a given host structure and frequency range [3].

Traditional transducer design methods rely on the use of the pin-force model [4–6], assuming that a piezoelectric actuator can be modelled as a constant shear stress applied at its edge, whatsoever the frequency generated. However, the assumptions behind this model are only valid for infinitely thin piezoelectric elements, for weak coupling between the host structure and the transducer and when the wavelength of the generated guided wave is above the size of the transducer. In practice, these assumptions are only verified at low frequencies (below 50 kHz) such that the design rules obtained using this model are usually not valid. Recently, a hybrid pin-force model [7] has been introduced by considering the complex shear stress profile at the interface between the actuator and the host structure. Improvements in terms of accuracy and bandwidth validity have been observed at the cost of a complete Finite Element Model (FEM) of the problem. An attempt to model the

detailed interaction of guided wave with piezoelectric actuator has been proposed [8, 9] by taking into account the complex in-plane shear stress distribution below the piezoceramic actuator under the plane strain assumption. However, the computational burden of this method and its moderate accuracy are limiting factors for practical implementation.

In the present paper, an analytical model is proposed for guided wave generation by a circular piezoceramic by taking into account the complex shear and normal stress profiles generated by the transducer. For this purpose, an analytical formulation is described and validated numerically using a Finite Element Model (FEM). The formulation is based on computation of the shear and normal stress distribution under the actuator when a voltage difference is applied between the two surface electrodes. The computed stress field is then used to predict the displacement field at a given distance. It is shown that the proposed model allows accurate prediction of in-plane and out-of plane velocity fields for both A_0 and S_0 modes over an extended bandwidth up to 1 MHz, while the pin-force model provides accurate prediction only for frequencies below 50 kHz.

1. ANALYTICAL MODEL FOR GUIDED WAVE GENERATION BY A CIRCULAR PIEZOCERAMIC

In the present paper, the guided wave generation by a circular piezoceramic or radius R and thickness h_p in an isotropic material of thickness $2h$ is considered as presented in Fig. 1.

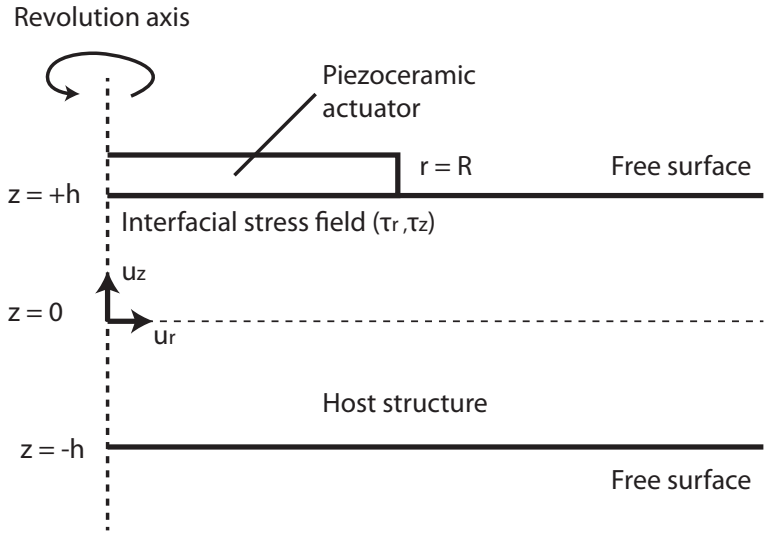

Figure 1 : Geometry used in the study.

In the absence of body forces, the equations of motion are defined by the Navier equation for the displacement field $\mathbf{u} = (u_r\ u_z)$:

$$(\lambda+\mu)\nabla(\nabla.\mathbf{u})+\mu\nabla^2\mathbf{u}=\rho\frac{\partial^2\mathbf{u}}{\partial t^2} \tag{1}$$

where (λ,μ) represent the Lamé coefficients and ρ the density of the considered material. The displacement field $\mathbf{u}$ can be decomposed as a vectorial irrotational potential $\mathbf{H}$ and a scalar potential Φ that satisfy:

$$\begin{cases} \mathbf{u}=\nabla\Phi+\nabla\times\mathbf{H} \\ \nabla.\mathbf{H}=0 \end{cases} \tag{2}$$

Defining the Hankel transform of orders 0 and 1 as follows [10]:

$$\bar{f}(k) = \int_0^\infty r f(r) J_0(kr) dr = \int_{-\infty}^\infty r f(r) H_0(kr) dr \tag{3}$$

$$\tilde{f}(k) = \int_0^\infty r f(r) J_1(kr) dr = \int_{-\infty}^\infty r f(r) H_1(kr) dr \tag{4}$$

where J_n and H_n denote bessel function and Hankel functions of order n. Looking at the harmonic solution using separated variables, i.e. $H(r,z,t) = H_r(r)H_z(z)e^{j\omega t}$ and $\Phi(r,z,t) = \Phi_r(r)\Phi_z(z)e^{j\omega t}$ at angular frequency ω, one obtains the following equations for Hankel transforms of wave potentials:

$$\left(\ddot{H}_z - \left(k^2 - \frac{\omega^2}{c_s^2}\right) H_z\right) \tilde{H}_r = 0 \tag{5}$$

$$\left(\ddot{\Phi}_z - \left(k^2 - \frac{\omega^2}{c_p^2}\right) \Phi_z\right) \bar{\Phi}_r = 0 \tag{6}$$

where $c_s = \sqrt{\frac{\mu}{\rho}}$ denotes the shear (S-) wave velocity and $c_p = \sqrt{\frac{\lambda+2\mu}{\rho}}$ represents the pressure (P-) wave velocity. Eqs 5 and 6 admit as a general solution in the $z-$ direction:

$$\Phi_z(z) = C_1 \cos \alpha z + C_2 \sin \alpha z \tag{7}$$

$$H_z(z) = C_3 \cos \beta z + C_4 \sin \beta z \tag{8}$$

with:

$$\alpha^2 = \frac{\omega^2}{c_p^2} - k^2 \qquad\qquad \beta^2 = \frac{\omega^2}{c_s^2} - k^2 \tag{9}$$

The Hankel transforms of the displacement field in the wavenumber domain can thus be expressed as:

$$\begin{pmatrix} \tilde{u_r} \\ \bar{u_z} \end{pmatrix} = \mathbf{U}.\mathbf{C} = (\mathbf{U_A} \mid \mathbf{U_S}).\begin{pmatrix} \mathbf{C_A} \\ \mathbf{C_S} \end{pmatrix} \tag{10}$$

where $\mathbf{C_A} = (C_2 C_3)'$ and $\mathbf{C_S} = (C_1 C_4)'$:

$$\mathbf{U_A} = \begin{pmatrix} -k\bar{\Phi}_r \sin \alpha z & \beta \tilde{H}_r \sin \beta z \\ \alpha \bar{\Phi}_r \cos \alpha z & k\tilde{H}_r \cos \beta z \end{pmatrix}, \quad \mathbf{U_S} = \begin{pmatrix} -k\bar{\Phi}_r \cos \alpha z & -\beta \tilde{H}_r \cos \beta z \\ -\alpha \bar{\Phi}_r \sin \alpha z & k\tilde{H}_r \sin \beta z \end{pmatrix} \tag{11}$$

The generalized Hooke's law in cylindrical coordinates can be written as:

$$\begin{pmatrix} \tilde{\sigma_{rz}} \\ \bar{\sigma_{zz}} \end{pmatrix} = \mu \ \ (\mathbf{S_A} \mid \mathbf{S_S}).\begin{pmatrix} \mathbf{C_A} \\ \mathbf{C_S} \end{pmatrix} \tag{12}$$

$$\mathbf{S_A}(z) = \begin{pmatrix} -2k\alpha\bar{\Phi}_r \cos \alpha z & (\beta^2 - k^2)\tilde{H}_r \cos \beta z \\ (k^2 - \beta^2)\bar{\Phi}_r \sin \alpha z & -2k\beta \tilde{H}_r \sin \beta z \end{pmatrix} \tag{13}$$

$$\mathbf{S_S}(z) = \begin{pmatrix} 2k\alpha\bar{\Phi}_r \sin \alpha z & (\beta^2 - k^2)\tilde{H}_r \sin \beta z \\ (k^2 - \beta^2)\bar{\Phi}_r \cos \alpha z & 2k\beta \tilde{H}_r \cos \beta z \end{pmatrix} \tag{14}$$

In the lower plate boundary, the free stress condition implies that $\tilde{\sigma_{rz}}(-h) = \bar{\sigma_{zz}}(-h) = 0$. On the upper plate boundary, the piezoceramics imposes not only a shear stress profile τ_r for $r < R$ but also a normal stress profile τ_z which is considered in the present study, such that the boundary condition can be written at both sides of the plate in $z = \pm h$:

$$\begin{pmatrix} \mathbf{S_A}(h) & \mathbf{S_S}(h) \\ \mathbf{S_A}(h) & -\mathbf{S_S}(h) \end{pmatrix} . \begin{pmatrix} \mathbf{C_A} \\ \mathbf{C_S} \end{pmatrix} = \begin{pmatrix} \tilde{\tau_r}/\mu \\ \bar{\tau_z}/\mu \\ 0 \\ 0 \end{pmatrix} \tag{15}$$

The final expression for the displacement field is obtained by extracting the values of the unknown vectors $\mathbf{C_A}$ and $\mathbf{C_S}$ based on the boundary conditions of Eq. 15:

$$\begin{pmatrix} \tilde{u_r} \\ \tilde{u_z} \end{pmatrix} = \frac{1}{2\mu} \left(\frac{\mathbf{N_A}(k,z,\omega)}{D_A(k,\omega)} + \frac{\mathbf{N_S}(k,z,\omega)}{D_S(k,\omega)} \right) \begin{pmatrix} \tilde{\tau}_r \\ \tilde{\tau}_z \end{pmatrix} \tag{16}$$

where:

$$D_S(k,\omega) = 4\alpha\beta k^2 \cos\beta h \sin\alpha h + (\beta^2 - k^2)^2 \sin\beta h \cos\alpha h \tag{17}$$

$$D_A(k,\omega) = 4\alpha\beta k^2 \sin\beta h \cos\alpha h + (\beta^2 - k^2)^2 \cos\beta h \sin\alpha h \tag{18}$$

and for displacement at the surface for $z = h$, this expression can be solved:

$$\mathbf{N_A}(k,h,\omega) = \begin{pmatrix} \beta(\beta^2+k^2)s_\alpha s_\beta & -k(k^2-\beta^2)s_\alpha c_\beta - 2\alpha\beta k c_\alpha s_\beta \\ -k(k^2-\beta^2)s_\alpha c_\beta - 2\alpha\beta k c_\alpha s_\beta & -\alpha(\beta^2+k^2)c_\alpha c_\beta \end{pmatrix} \tag{19}$$

$$\mathbf{N_S}(k,h,\omega) = \begin{pmatrix} -\beta(\beta^2+k^2)c_\alpha c_\beta & -k(k^2-\beta^2)c_\alpha s_\beta - 2\alpha\beta k s_\alpha c_\beta \\ -k(k^2-\beta^2)c_\alpha s_\beta - 2\alpha\beta k s_\alpha c_\beta & \alpha(\beta^2+k^2)s_\alpha s_\beta \end{pmatrix} \tag{20}$$

with:

$$c_\alpha = \cos\alpha h, \qquad s_\alpha = \sin\alpha h, \qquad c_\beta = \cos\beta h, \qquad s_\beta = \sin\beta h \tag{21}$$

The displacement fields at a propagating distance r are then obtained using inverse Hankel transform for $r > 0$ and integration using the residue theorem in order to obtain the following expression:

$$\begin{aligned} \begin{pmatrix} u_r \\ u_z \end{pmatrix} &= \begin{pmatrix} H_1^{(2)}(k_A r) & 0 \\ 0 & H_0^{(2)}(k_A r) \end{pmatrix} \frac{k_A \mathbf{N_A}(k_A,z,\omega)}{D'_A(k_A,\omega)} \begin{pmatrix} \tilde{\tau}_r(k_S) \\ \tilde{\tau}_z(k_S) \end{pmatrix} \\ &+ \begin{pmatrix} H_1^{(2)}(k_S r) & 0 \\ 0 & H_0^{(2)}(k_S r) \end{pmatrix} \frac{k_S \mathbf{N_S}(k_S,z,\omega)}{D'_S(k_S,\omega)} \begin{pmatrix} \tilde{\tau}_r(k_S) \\ \tilde{\tau}_z(k_S) \end{pmatrix} \end{aligned} \tag{22}$$

where $D'_A(k_A,\omega)$ denotes the derivative of $D_A(k,\omega)$ with respect to k at $k = k_A$. In Eqs. 19 and 20, the non-diagonal terms are equal, suggesting that the influence of interfacial shear stress on out-of plane component is equal to the contribution of normal stress on in-plane displacement. In Eq. 22, the generation of guided waves is directly related by the Hankel transforms of order 0 of the surfacial normal stress field $\tilde{\tau}_z(k)$ and the Hankel transform of order 1 of the interfacial shear stress $\tilde{\tau}_r(k)$ between the piezoecramic actuator and the plate. In the following section, the evolution of this interfacial stress profiles with respect to host structure, piezoceramic thickness, and frequency is studied numerically.

2. NUMERICAL VALIDATION

2.1 Finite Element Model description

In order to compute the interfacial stress profile, a FEM has been developed under COMSOL v4.3. In order to perform the simulation with a conventional workstation (Intel Dual Core 2 GHz - 2 Gb of RAM), a 2.5-D axi-symmetric model has been developed in the frequency domain for frequencies below 1 MHz. The area of interest is 100 mm long and includes the host structure, piezoceramic transducers and absorbing regions. The simulations are performed in the frequency domain assuming continuous harmonic wave excitation. An absorbing layer is modelled around the area of interest to ensure an infinite plate condition by adding an imaginary part to the elastic constants that increases with respect to the propagation distance [11]. The piezoceramic is assumed perfectly bonded on the host plate and a harmonic input voltage of 1V is used as an excitation signal.

A number of 10 nodes per minimal wavelength for A_0 mode is ensured by setting the maximal mesh size at 0.25 mm in the targeted area. Local strong mesh refinement around the piezoceramic edges has been used. Quadratic triangular elements are used for a total of approximatively 10^5 elements. Post-processing is performed using MATLAB and computation of the piezoceramic impedance and transfer function between piezoceramic actuator and surface displacement is extracted.

Simulations are performed for a 1.5 mm thick aluminium plate (Young's modulus of 70 GPa, Poisson's ratio of 0.33 and density of 2700 kg/m^3) and for a PZT-5A piezoceramic actuator with a thickness of 0.5 mm and a radius of R=5 mm.

2.2 Influence of normal stress on guided wave generation by a circular piezoceramic

In this, section, the validation of the propagation model is investigated on a reference case for which a R=5 mm radius piezoceramic of thickness h_p=0.5 mm is mounted of a 1.5 mm thick aluminium plate. Fig. 2.2 presents the amplitude of the shear and normal stress fields below the piezoceramic actuator.

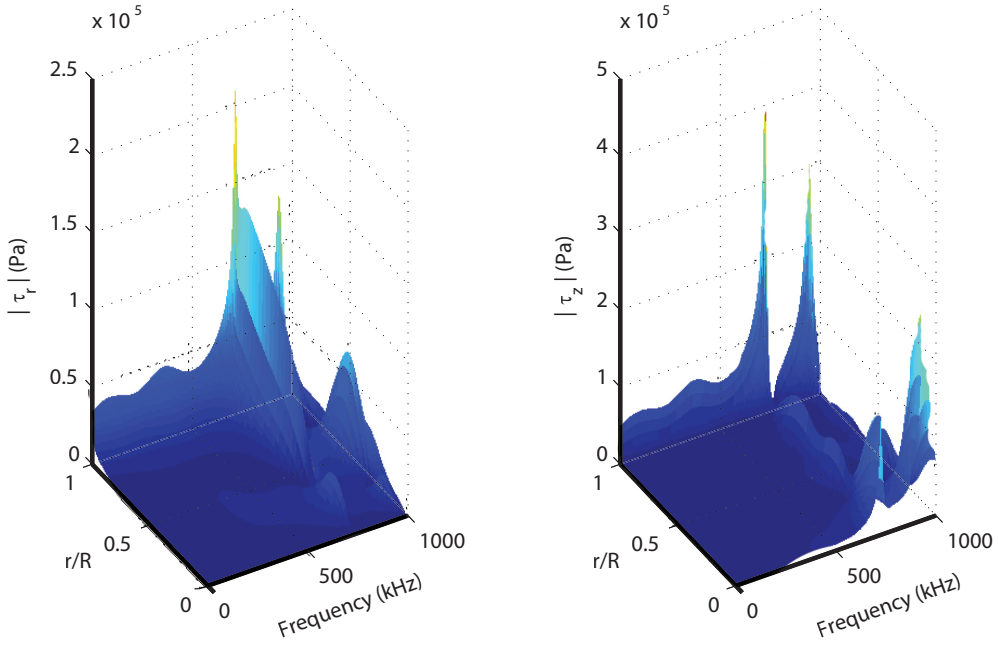

Figure 2 : Amplitude of the interfacial shear (left) and normal (right) stress profiles as a function of frequency and radius.

Concerning the shear stress profile, a divergent behaviour appears for frequencies below 300 kHz at the tip of the actuator (i.e. for r=R) as predicted by the pin-force model. For higher frequencies, the mechanical resonances of the piezoceramic actuator are responsible for more complex shear stress distribution which is no longer concentrated at the tip of the actuator. In Fig. 2.2, it appears that the amplitude of normal and shear stresses are of the same order of magnitude, such that the contribution of normal stress on the guided wave generation can no longer be neglected. Below the first mechanical resonance (around 300 kHz), the normal stress profile is similar to the shear stress profile but large variations are observed for frequencies above the first mechanical resonance.

Fig. 2.2 presents the computed surface displacement field for both in-plane and out-of plane components for an observer located at r=25 mm (5R) for both symmetric and antisymmetric modes. In each case, the FEM solution (points) is compared to the analytical solution described in Eq. 22 when considering shear stress only (dotted line) and both normal and shear stresses components (solid line). An excellent fit is observed between the numerical model and the analytical solution when considering both stress components. However, when considering the shear stress only, both in- and out-of plane components of anti-symmetric displacement field are badly estimated, confirming the necessity of taking into account the normal stress contribution.

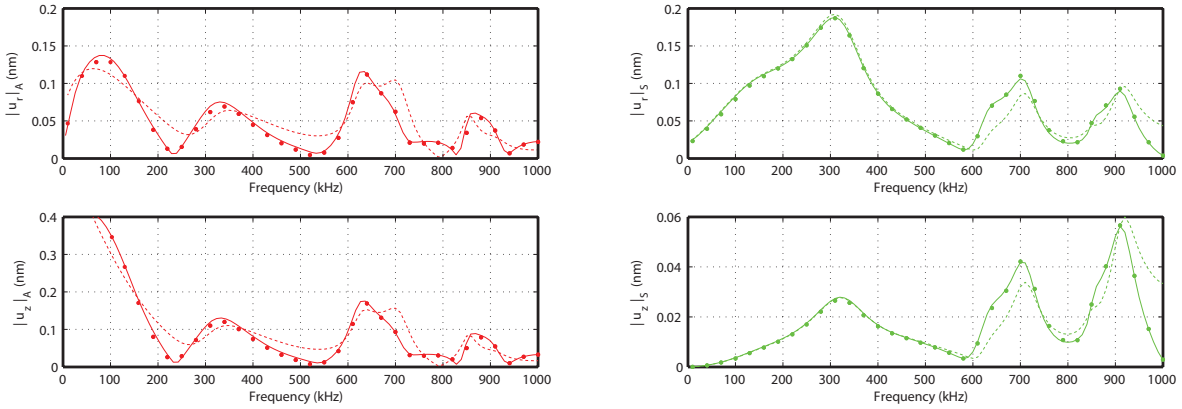

Figure 3 : Amplitude of the surface in-plane (top) and out-of-plane (bottom) displacement field at a distance of 25 mm (5 R) for antisymmetric (left) and symmetric modes (right). In each case, the FEM solution (points) is compared to the analytical solution considering shear stress only (dotted line) and both normal and shear stresses (solid line).

2.3 Approximation of the excitation functions

As described in Eq. 22, the excitation terms are represented by the Hankel transforms of the surfacial shear and normal stress fields at propagating wavenumbers k_A and k_S. Thus, the determination of the exact stress profile is not required for guided wave generation estimation but only the projection on S_0 and A_0 modes is required (one complex value per frequency). Thus, depending on the host structure and piezoceramic characteristics, the total displacement field in the host structure can be reconstructed by computing for $k = k_A$ or $k = k_S$:

$$\tilde{\tau}_r(k) = \int_0^R rJ_1(kr)\tau_r(r)dr \tag{23}$$

$$\tilde{\tau}_z(k) = \int_0^R rJ_0(kr)\tau_z(r)dr \tag{24}$$

Considering a pure shear stress field concentrated at the tip of the actuator (pin-force assumption), those equations can be reduced:

$$\tau_r^{PF}(r) = \tau_{0r}\delta(R), \qquad \tilde{\tau}_r^{PF}(k) = \tau_{0r}RJ_1(kR) \tag{25}$$

$$\tau_z^{PF}(r) = \tau_{0z}\delta(R), \qquad \tilde{\tau}_z^{PF}(k) = \tau_{0z}RJ_0(kR) \tag{26}$$

which only consider the radius R of the actuator as a parameter. In order to consider mechanical resonances and more complex shear stress evolution, we propose a refined model by approximating

the functions $\bar{\tau}_z(k)$ and $\tilde{\tau}_z(k)$ using:

$$\tau_r^M(r) = \tau_{0r}\delta(R) + A(w)\tau_{1r}r, \qquad \tilde{\tau}_r^M(k) = \tau_{0r}RJ_1(kR) + A(w)\tau_{1r}RJ_2(kR)/k \tag{27}$$

$$\tau_z^M(r) = \tau_{0z}\delta(R) + A(w)\tau_{1z}, \qquad \bar{\tau}_z^M(k) = \tau_{0z}RJ_0(kR) + A(w)\tau_{1z}RJ_1(kR)/k \tag{28}$$

where $A(w)$ denotes an amplitude correction factor containing the contribution of mechanical resonances of the piezoceramic actuator. In practice, the function $A(w)$ can be approximated by the real part of the measured admittance. Fig. 2.3 presents the evolution of $\bar{\tau}_z$ and $\tilde{\tau}_r$ for A_0 and S_0 modes and compares the FEM solution to the pin-force model and the proposed model. In each case, the functions $\tau_{0r}, \tau_{0z}, \tau_{1r}$ and τ_{1z} are estimated via minimization algorithms.

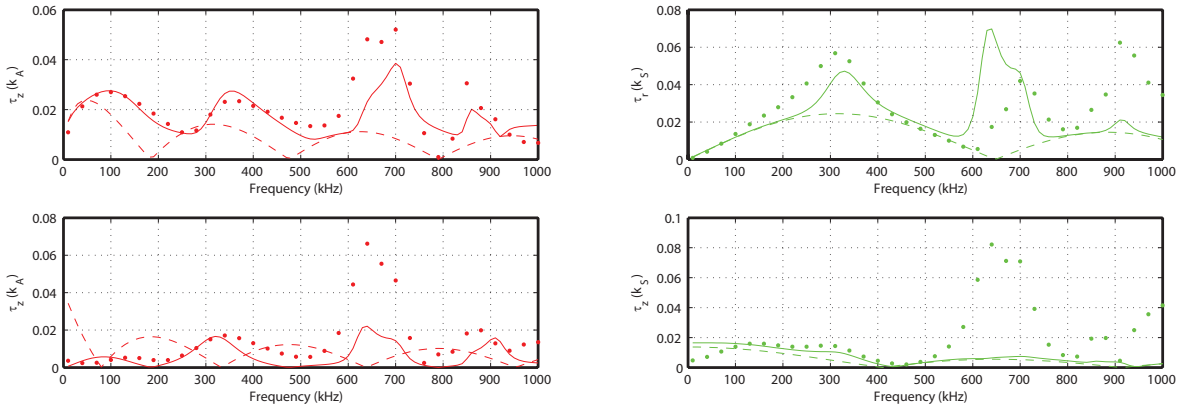

Figure 4 : Excitation terms $\tilde{\tau}_r(k)$ (top) and $\bar{\tau}_z(k)$ (bottom) for A_0 (left) and S_0 (right) modes. In each case, the exact solution (FEM - dots) is compared to the pin-force model (dashed) and proposed model (solid line).

In this figure, it appears that the pin-force model is limited to frequencies below 50 kHz for which the dynamics of the piezoceramic can be neglected. Above 50 kHz, the proposed model allows taking into account the first mechanical resonance around 300 kHz and increases. Above 500 kHz, the second mechanical resonance is not modelled with the proposed formulation, explaining the differences between the FEM results and the proposed model.

CONCLUSION

In this paper, a three-dimensional model of guided wave generation by a circular piezoceramic is proposed, taking into account the complex shear and normal interfacial stress profile between the transducer and the host structure. The complex stress profile is extracted from a FEM and then used as a parameter in the analytical formulation. The influence of piezoceramic actuator dimension, thickness and host structure properties is assessed numerically and an empirical model for guided wave generation terms is proposed. Extension in the case of higher order modes of the actuator is in progress.

ACKNOWLEDGEMENTS

The authors would like to thank the Natural Sciences and Engineering Research Council of Canada (NSERC) fro its financial support.

REFERENCES

[1] C.R. Farrar and K. Worden. An introduction to structural health monitoring. *Philosophical Transactions of the Royal Society*, 365:303–315, 2007.

[2] N.Quaegebeur, P.-C. Ostiguy, and P. Masson. Correlation-based imaging technique for fatigue monitoring of riveted lap-joint structure. *Smart Materials and Structures*, 23(5):055007, 2014.

[3] N. Quaegebeur, P. Micheau, P. Masson, and M. Castaings. Methodology for optimal configuration in structural health monitoring of composite bonded joints. *Smart Materials and Structures*, 21(10):105001, 2012.

[4] A. Raghavan and C.E.S. Cesnik. Finite-dimensional piezoelectric transducer modeling for guided wave based structural health monitoring. *Smart Materials And Structures*, 14:1448–1461, 2005.

[5] H. Sohn and S.J. Lee. Lamb wave tuning curve calibration for surface-bonded piezoelectric transducers. *Smart Materials And Structures*, 19:1–12, 2010.

[6] L. Yu, G. Bottai-Santoni, and V. Giurgiutiu. Shear lag solution for tuning ultrasonic piezoelectric wafer active sensors with applications to Lamb wave array imaging. *International Journal of Engineering Science*, 48(10):848–861, 2010.

[7] P.-C. Ostiguy, N. Quaegebeur, and P. Masson. Improved damage imaging in aerospace structures using a piezoceramic hybrid pin-force wave generation model. In *SPIE conference, San Diego*, 2014.

[8] G.L. Huang and C.T. Sun. The dynamic behaviour of a piezoelectric actuator bonded to an anisotropic elastic medium. *International Journal of Solids and Structures*, 43(5):1291 – 1307, 2006.

[9] XD Wang and GL Huang. Wave propagation in electromechanical structures: induced by surface-bonded piezoelectric actuators. *Journal of Intelligent Material Systems and Structures*, 12(2):105–115, 2001.

[10] M.S. Wengrovitz, A.V. Oppenheim, and G.V. Frisk. Reconstruction of complex-valued propagating wave fields using the hilbert-hankel transform. *JOSA A*, 4(1):247–266, 1987.

[11] B. Hosten and M. Castaings. Finite elements methods for modeling the guided waves propagation in structures with weak interfaces. *The Journal of the Acoustical Society of America*, 117(3):1108–1113, 2005.